

## Surface Defect Sites Formed on Partially and Fully Dehydrated MgO: An EPR/ENDOR Study

Damien M. Murphy,\* Robert D. Farley, Ian J. Purnell, Christopher C. Rowlands, and Abdul R. Yacob†

National EPSRC ENDOR Centre, Department of Chemistry, University of Wales Cardiff, Cardiff CF1 3TB, United Kingdom

Maria Cristina Paganini and Elio Giamello

Dipartimento di Chimica IFM, Università di Torino, Via P. Giuria 9, 10125 Torino, Italy

Received: October 22, 1998; In Final Form: January 12, 1999

EPR and ENDOR spectroscopy have been used to investigate a variety of trapped electron centers on the surface of polycrystalline MgO. The oxide was dehydrated under vacuum at different temperatures (673–1123 K) and UV irradiated under H<sub>2</sub>. The dehydration process results in the formation of surface anion vacancies, which subsequently act as excess electron traps (forming color centers). A variety of such color centers have been identified. At high activation temperatures (1123 K), surface F<sub>S</sub><sup>+</sup>(H) color centers (type I) are formed, which have been assigned to an electron trapped by a specific anion vacancy. At slightly lower activation temperatures, a second F<sub>S</sub><sup>+</sup>(H) color center (type II) predominates; this center has been assigned to an electron trapped in a higher coordinated surface vacancy. However, at low activation temperatures such that the oxide surface remains partially hydrated, different types of color centers are present. It is proposed that these centers arise from electron trapping at a surface cation–anion vacancy pair (tentatively assigned as P<sub>S</sub><sup>−</sup> centers). The mechanism by which the latter center is effectively reduced by a single electron is unclear. The distribution and abundance of these different trapped electron centers varies as a function of the dehydration temperature. The results show that the surface of polycrystalline MgO containing a variety of point defects changes dramatically depending on the pretreatment conditions.

### Introduction

Pure and doped polycrystalline MgO powders are good catalysts for many chemical reactions.<sup>1</sup> Nevertheless, knowledge about the actual catalytic sites or surface defects responsible for the reactivity is often imprecise and poorly understood. Although the surface properties of magnesium oxide have been studied in great depth both experimentally and theoretically, a great many questions remain unanswered. One such question concerns the collective problem associated with the nature, location, and abundance of the surface anion vacancies and the processes by which they are formed during surface dehydration.

Significant theoretical advances using atomistic simulations, quantum chemical calculations, and *ab initio* calculations have recently been made in an attempt to understand the nature of the irregular and defective faces of oxides and the molecular processes occurring at these defects.<sup>2–13</sup> Anion and cation vacancies on fully dehydrated MgO surfaces have received considerable attention of late. In particular, a variety of point defects such as oxygen vacancies (F centers), magnesium vacancies (V centers), simple aggregates of defects (the divacancy or P center), and in some cases migration of these defects have been simulated both in the bulk<sup>5</sup> and at the surface of MgO.<sup>6–11</sup> While many of these studies have provided valuable

insights into the geometric structure and electronic properties of the vacancies themselves on the dehydrated surfaces, the dynamics by which these defects form under real conditions has not been treated in depth. Many studies have been performed on the adsorption of water on oxides and on the nature of the hydrated MgO surface,<sup>12–15</sup> and the results clearly show a strong preference for hydroxylation at the low coordination sites. It has been shown from experiments that thermal dehydration is not a simple reversal of ambient temperature hydration, particularly during the last stages of dehydration where some surface reconstruction occurs.<sup>16</sup> Nevertheless, to the best of our knowledge, there is no clear theoretical study on the relationship between the state of surface dehydroxylation and the creation of surface defects.

From an experimental viewpoint, it is well-known that the pretreatment conditions, such as the temperature of calcination and the extent of surface dehydration, significantly affect the surface morphology and defectivity of the oxide.<sup>17–19</sup> Significant attention has therefore been given to the role of the hydroxyl groups in the mechanism of surface hydration and dehydration, since these processes are ultimately responsible for the creation of surface sites active in the adsorption and catalytic behavior of MgO.<sup>19–21</sup> Dehydroxylation of the polycrystalline MgO surface was followed by TPD and specific peaks ascribed to energetically different forms of adsorbed water and OH groups which were removed only at elevated temperatures.<sup>16</sup> Coluccia et al.<sup>22–24</sup> used IR and photoluminescence spectroscopy to follow

\* Author for correspondence.

† Permanent address: Universiti Teknologi Malaysia, Karung Berkunci 791, 80990 Johor Bahru, Negeri Johor Darul Ta'zim, Malaysia.

the dehydroxylation of magnesia surfaces and demonstrated that dehydration occurs in a successive manner starting from the condensation between neighboring and weakly bound OH groups, probably from the (001) face, and ending with the tightly bound hydroxyl groups at low coordinated surface positions. Removal of water at these latter stages of dehydroxylation occurs at the expense of a lattice  $\text{O}^{2-}$  anion and the resulting formation of a surface vacancy. Because the removal and corresponding reconstruction of the surface at the final stage of dehydration occurs at unsaturated positions, the final anion vacancies can also be viewed as low coordinated. The experimental evidence, although indirect, is therefore clear; anion vacancies are created on magnesia surfaces activated at high temperatures.

Experimentally, the surface anion vacancies (formally labeled  $\text{F}_\text{S}^{2+}$  due to the absence of the divalent negative charge from  $\text{O}^{2-}$ ) are difficult to observe, often invisible to many surface science techniques. However, their existence can be shown by doping the vacancy with an excess electron; the one electron reduced defect or  $\text{F}_\text{S}^+$  color center is paramagnetic and can then be studied either by EPR or DR UV-vis spectroscopy. One can then obtain information on the nature and type of defect that existed before the electron was trapped. In a series of previous investigations, we have studied the spectroscopic features of the surface color centers on dehydrated alkaline earth oxides, predominantly by EPR.<sup>25–28</sup> We examined in depth the magnetic and electronic properties of the  $\text{F}_\text{S}^+(\text{H})$  center in order to understand the location of this defect on the surface. This particular color center is formed by UV irradiation of the thoroughly dehydrated surface in the presence of adsorbed  $\text{H}_2$ ; the surface adsorbs the molecule heterolytically and the resulting  $\text{H}^-$  species are photolyzed to release their electrons so the final  $\text{H}^+$  becomes stabilized on a surface  $\text{O}^{2-}$  anion (forming OH) in close proximity to the  $\text{F}_\text{S}^+$  center. The model of the  $\text{F}_\text{S}^+(\text{H})$  center originally proposed by Tench and Nelson<sup>29–31</sup> regarded this defect as located on the flat (001) face. This hypothesis was recently scrutinized by some of us and, based on combined EPR, DR UV-vis, FTIR, and quantum chemical calculations, it was found that the defect actually exists on very low coordinated surface positions.<sup>28</sup>

As described above, the majority of the studies to date have focused on the nature of the defect centers formed on the fully dehydrated magnesia surface. Few studies have been performed on the more complex factors related to surface defects formed on partially dehydrated MgO. Generally, high surface area MgO can be prepared by dehydroxylation of the hydroxide ( $\text{Mg}(\text{OH})_2$ ) under vacuum. As the hexagonal structured hydroxide is systematically converted to the cubic oxide, a variety of different point defects can be formed in the bulk and at the surface. Certainly at the last stages of surface dehydroxylation, as described above, the high-temperature activated oxide contains numerous anion vacancies formed at low coordinated surface sites. However, a large number of other point defects are also created at a slightly lower temperature in which the oxide remains partially hydrated. Lunsford and Jayne<sup>18</sup> identified, for example, a large number of surface color centers that also existed on partially dehydrated MgO (873–973 K). But the current ideas on surface dehydroxylation do not accommodate the possibility that defects are formed on the partially hydrated materials. The nature of these defects and their relation if any to the anion vacancies that form at the higher activation temperatures is uncertain.

The purpose of the current paper is to investigate the nature of the surface defects created on MgO in the temperature range 673–1123 K using EPR and ENDOR (electron nuclear double

resonance) spectroscopy. ENDOR has been used for many years to study trapped hole and trapped electron defects in solids,<sup>32</sup> including aggregates of F centers and  $\text{OH}^-$  molecules ( $\text{F}_\text{H}(\text{OH})^-$ ) centers in KBr.<sup>33</sup> However, there has not been any extensive use of the technique to probe surface defect states. Because the anisotropy of the surface color centers is quite small and often poorly resolved in the EPR spectrum due to the heterogeneous polycrystalline nature of the sample, ENDOR will provide further resolution on the magnetic properties of the surface color centers. In particular, it will be shown that a distribution of surface color centers (and vacancies) are created at different activation temperatures.

## Experimental Section

Commercial magnesium oxide (ex Johnson Matthey) was converted into the hydroxide ( $\text{Mg}(\text{OH})_2$ ) by overnight treatment in distilled water at 333 K. At this temperature, the oxide is hydrolyzed to the hydroxide. The hydroxide (~15 mg) was loaded into a quartz cell, which also contained the EPR tube, and slowly decomposed under vacuum at 523 K to obtain high surface area (HSA) MgO. The oxide was then activated under vacuum ( $10^{-5}$  Torr) at selected temperatures (673, 773, 873, 973, 1023, 1048, 1073, and 1123 K) for about 1 h. After these dehydration treatments, the activated oxide was cooled to room temperature, exposed to hydrogen (100 Torr), and UV irradiated at 298 or 100 K. After 15 min of irradiation, the sample developed a deep-blue coloration, indicating the formation of surface color centers.

A 1 kW Oriel Instruments UV lamp, incorporating a Hg/Xe arc lamp (250 nm to >2500 nm), was used for all irradiations, in conjunction with a water filter. The UV output below 280 nm accounts for only 4–5% of the total lamp output. The EPR/ENDOR spectra were recorded on a CW X-band Bruker ESP 300E series spectrometer equipped with an ESP360 DICE ENDOR unit, operating at 12.5 kHz field modulation in a Bruker ER 200 ENB cavity. All spectra (EPR and ENDOR) were recorded at 100 K; the ENDOR spectra were obtained at 4 mW microwave power, 8 dB RF power from a ENI A-300 RF amplifier, and 199 kHz RF modulation depth, again at 12.5 kHz modulation frequency.

## Results

### MgO Dehydrated in the Temperature Range 1023–1123 K.

Figure 1a–d shows a series of EPR spectra of MgO activated at different temperatures (1023, 1048, 1073, and 1123 K, respectively) and UV irradiated at 100 K under hydrogen. All samples developed a blue coloration immediately after irradiation. The profile of the EPR spectra changes quite dramatically as the activation temperature of the oxide is varied. At the lowest temperature examined in this series (1023 K), a broad and rather poorly resolved signal centered at  $g \approx 2.0005$  can be observed (Figure 1a). As the activation temperature is increased, however, the resolution and apparent complexity of the signal changes (Figure 1b). At the highest activation temperature (1123 K), a well-resolved spectrum is observed with a characteristic doublet hyperfine splitting (Figure 1d) known to arise from a magnetic interaction between the trapped electron and a neighboring OH group. This previously reported EPR signal has been assigned to the surface  $\text{F}_\text{S}^+(\text{H})$  center<sup>25–31</sup> and will be discussed in detail below.

The corresponding ENDOR spectra for each sample are shown in Figure 2a–d. The spectra were recorded at the central magnetic field position marked A in Figure 1d (i.e., producing a powder-like ENDOR spectrum, containing contributions from

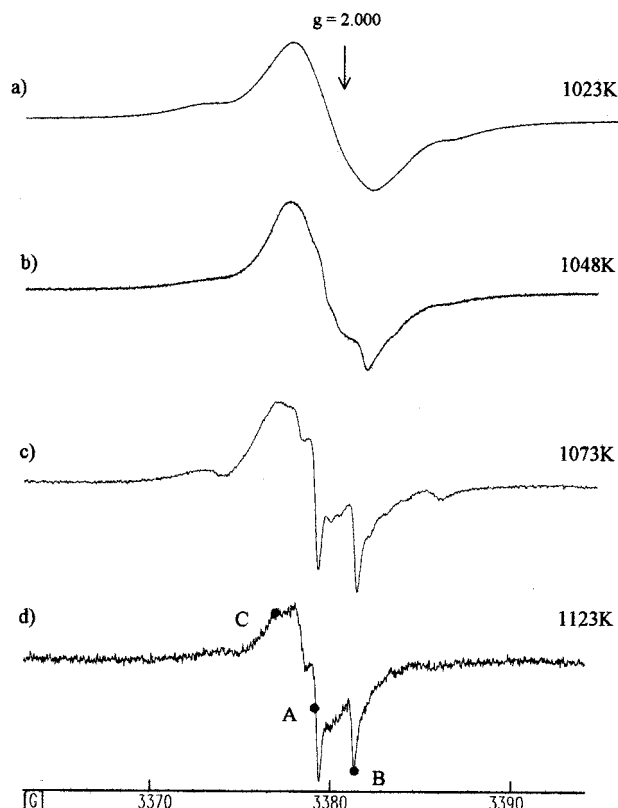


**Figure 1.** EPR spectra recorded at 100 K of surface  $F_S^+(H)$  centers on MgO dehydrated at (a) 1023 K, (b) 1048 K, (c) 1073 K, and (d) 1123 K. The field positions marked A, B, and C indicate where the  $^1H$  ENDOR spectra were measured.

many orientations of the powder sample). ENDOR spectra were also recorded at the higher field position marked B (Figure 1) so that the magnetic field vector lies in the plane of the perpendicular component of the hyperfine tensor. The magnitude of the  $^1H$  couplings do not change when the field is moved from position A to B (as expected when many orientations are selected), and more importantly, since the intensity of the ENDOR signal was greater for spectra recorded at position A, it was decided to measure all couplings at this central position. The ENDOR spectra are dominated by a central feature centered on the  $^1H$  nuclear frequency ( $\nu_H = 14.9$  MHz) which decreases in intensity as the dehydration temperature increases. This feature is due to the background  $^1H$  “matrix” signal arising from long-range couplings to distant protons, which is expectedly larger at the lower temperatures with higher concentrations of residual surface OH groups. The peak marked with the asterisk in Figure 2d is unaccounted for but likely due to an impurity, as the intensity varies significantly from one sample to the next, and may possibly be due to  $^{19}F$  “matrix” line.

Figure 1d is peculiar in this series of ENDOR spectra since it contains only one  $^1H$  coupling (labeled I), characterized by a pair of lines with a coupling of 5.715 MHz. A poorly resolved parallel coupling of 0.866 MHz was also observed when the magnetic field was set at position C (spectrum not shown). The measured  $^1H$  couplings correspond well with the observed splitting in the EPR spectrum (Figure 1d) and can be regarded as the first ENDOR spectrum of the surface  $F_S^+(H)$  center. Further analysis of the low-frequency  $^1H$  ENDOR line at 11.75 MHz over a wider sweep width and higher amplification (see insert of Figure 2c) reveals a slight asymmetry of the line, which indicates the presence of two overlapping signals. Although the A tensor measured from the EPR spectrum appears axial with

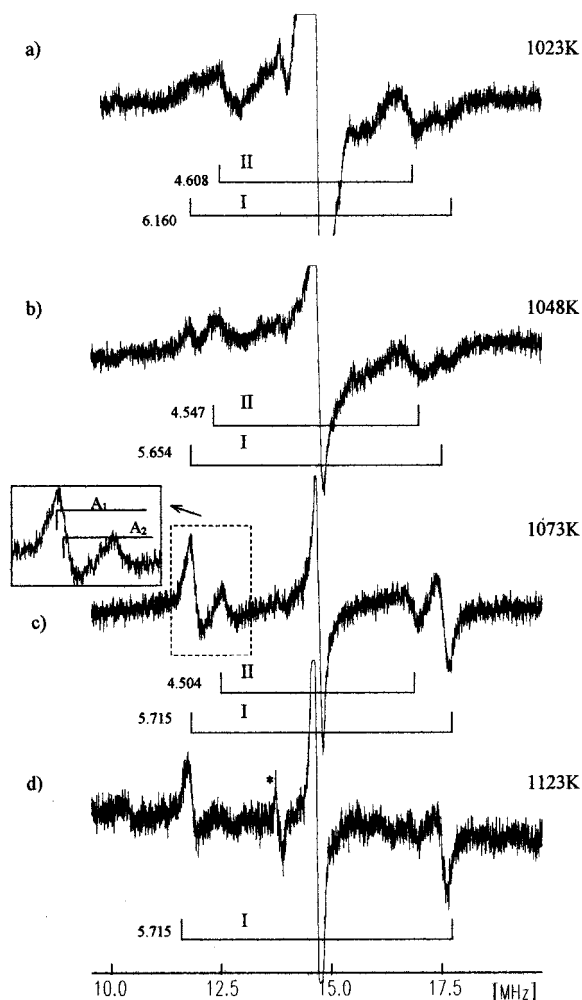


**Figure 2.**  $^1H$  ENDOR spectra recorded at 100 K of the color centers on MgO dehydrated at (a) 1023 K, (b) 1048 K, (c) 1073 K, and (d) 1123 K. The ENDOR spectra were taken at the magnetic field position marked A in Figure 1.

**TABLE 1: Spin Hamiltonian Parameters for the Paramagnetic Color Centers Formed on Magnesium Oxide after Dehydration at Various Temperatures**

species	$g_{\perp}$	$g_{\parallel}$	$A_{\perp}/\text{MHz } (^1H)$	$A_{\parallel}/\text{MHz } (^1H)$	$T^b/\text{K}$
$F_S^+(H)$ I	1.9994	2.001	5.799, 5.617	0.866	1123
$F_S^+(H)$ II	2.0000	2.0013	4.504	$\sim 0.8$	1048
$P_S^-$	2.0005	2.0016			873
$F_{SS}^+$	$g_{iso} = 2.0028$				573

<sup>a</sup> “P” center indicates a neutral cation–anion divacancy pair, based on nomenclature adopted in the literature.<sup>5,10</sup> The “s” subscript indicates a surface center, and the trapping of one electron gives the center the overall negative charge. <sup>b</sup> Approximate temperatures at which the specified color center is most abundant.

$A_{\perp} \approx 5.8$  MHz, the extra resolution provided by ENDOR reveals a nonaxial  $^1H$  A tensor with  $A_1 = 5.799$  MHz,  $A_2 = 5.617$  MHz, and  $A_3 = 0.866$  MHz (see Table 1).

At the slightly lower activation temperatures, an additional pair of lines labeled II can be detected (1073 K; Figure 2c) of magnitude 4.504 MHz (Table 1). The intensity of this second  $^1H$  signal grows as the activation temperature is lowered and is accompanied by a slight increase in the observed coupling from 4.504 MHz at 1073 K to 4.547 and 4.608 MHz at 1048 and 1023 K, respectively (Figure 2, parts b and a). Simultaneously, the former  $F_S^+(H)$  coupling I (5.715 MHz) diminishes slightly in intensity and appears only as a shoulder on the second

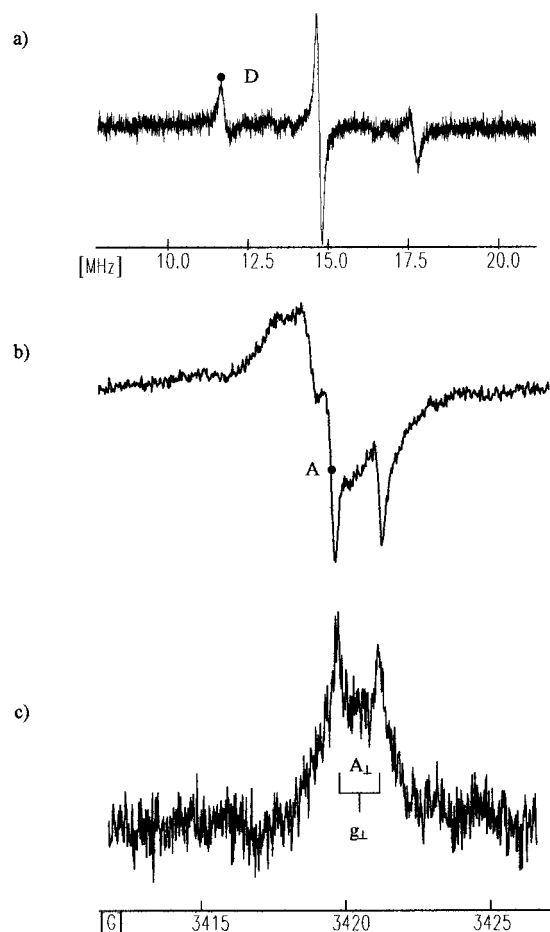


**Figure 3.** (a)  $^1\text{H}$  ENDOR and (b) EPR spectra of an  $\text{F}_\text{S}^+(\text{H})$  center on MgO dehydrated at 1123 K. (c) ENDOR-induced EPR spectrum, measured at the position marked D.

coupling II at the lower activation temperatures (Figure 2a). The two couplings I and II are not related, since their relative intensities vary independently from one experiment to the next. The latter coupling II can therefore be assigned to a second surface color center (hereafter labeled  $\text{F}_\text{S}^+(\text{H})$  II).

The above ENDOR spectra are most informative since they reveal the presence of a second surface color center normally hidden in the EPR spectrum. For example, the EPR spectra shown in parts c and d of Figure 1 are quite similar, despite the substantial contribution from the second  $\text{F}_\text{S}^+(\text{H})$  II center in Figure 1c. As this contribution increases (Figure 1, parts a and b), the expected increased complexity of the EPR spectrum is not usually observed; only an increased line width is seen. Care must therefore be taken in the assignment of broad EPR spectra from color centers to a single species, as several different centers may contribute to a complex and broad signal which can only be accurately analyzed by ENDOR. This effect is further illustrated in Figures 3 and 4 which show a typical ENDOR, EPR, and EIE (ENDOR-induced EPR) spectra of MgO dehydrated at 1123 and 1073 K, respectively. The ENDOR spectrum in Figure 3a was measured at the magnetic field position A in Figure 3b. The EIE spectrum was obtained by locking the RF field exactly at position D in Figure 3a while the magnetic field was swept. Under these conditions, a "single-crystal-type" EPR spectrum is obtained which clearly reveals the presence of only one  $^1\text{H}$  coupling. When the analogous experiment is repeated (Figure 4) on the lower activated oxide (MgO  $T_{\text{dehy}} = 1073$  K), the EPR spectrum (Figure 4b) is resolved into the individual  $^1\text{H}$  couplings as seen in the ENDOR spectrum (Figure 4a); the

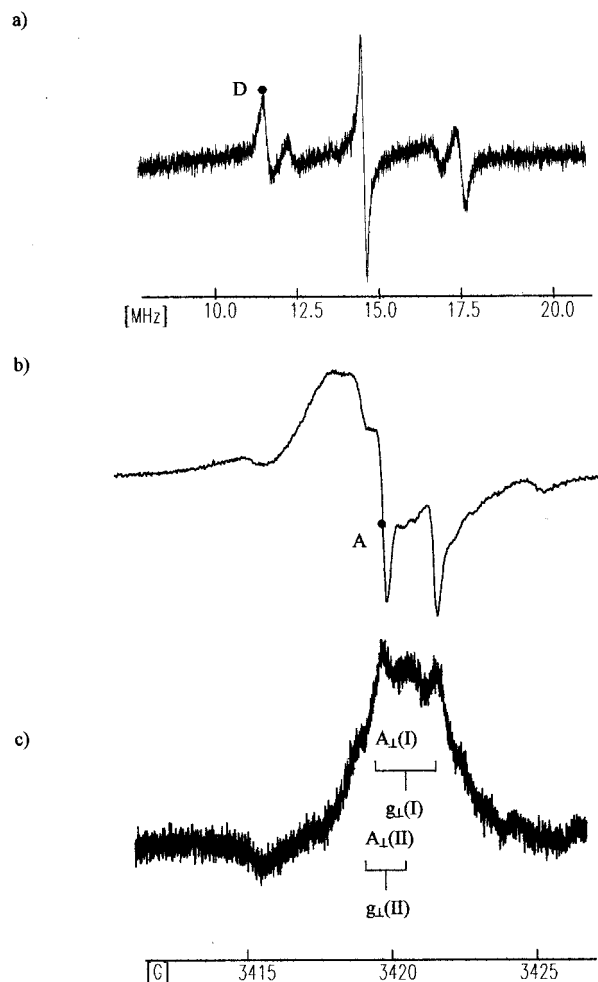


**Figure 4.** (a)  $^1\text{H}$  ENDOR and (b) EPR spectra of an  $\text{F}_\text{S}^+(\text{H})$  center on MgO dehydrated at 1073 K. (c) ENDOR-induced EPR spectrum, measured at the position marked D.

final EIE demonstrates how the  $g_\perp$  is normally complicated by the two superimposed doublets from  $\text{F}_\text{S}^+(\text{H})$  I and II.

The above results clearly show the following: (1) following dehydration at 1123 K one dominant surface color center ( $\text{F}_\text{S}^+(\text{H})$  I) exists on polycrystalline magnesium oxide; (2) at slightly lower dehydration temperatures, a second surface color center is formed ( $\text{F}_\text{S}^+(\text{H})$  II); (3) the latter center (II) is more abundant at the lower dehydration temperatures.

#### MgO Dehydrated in the Temperature Range 673–973 K.

Once the dehydroxylation temperature decreases below about 1023 K, there is a very marked difference in the profile of the EPR/ENDOR spectra compared to the former spectra on the high-temperature activated oxide (Figures 1 and 2). Figure 5a–d shows the EPR spectra of UV-irradiated MgO (in the presence of  $\text{H}_2$ ) after dehydration of the oxide at 673, 773, 873, and 973 K, respectively. The EPR spectra are now composed of two distinct and separate signals with  $g$  values of 2.0028 and 2.000. The former signal (marked with the asterisk in Figure 5) was previously reported on MgO<sup>18,25,26</sup> and has been assigned<sup>25</sup> to a subsurface paramagnetic  $\text{F}^+$  center.

The second signal characterized by the broad resonance at  $g \approx 2.000$  in Figure 5 can be assigned to a paramagnetic surface F-type color center.<sup>18,25,26</sup> This assignment is based on the following: (a) all the MgO samples, regardless of their hydration degree, are pale blue in color after irradiation (indicative of color center formation); (b) the resonant field position of the signal is typical of surface trapped electrons (i.e., small and negative



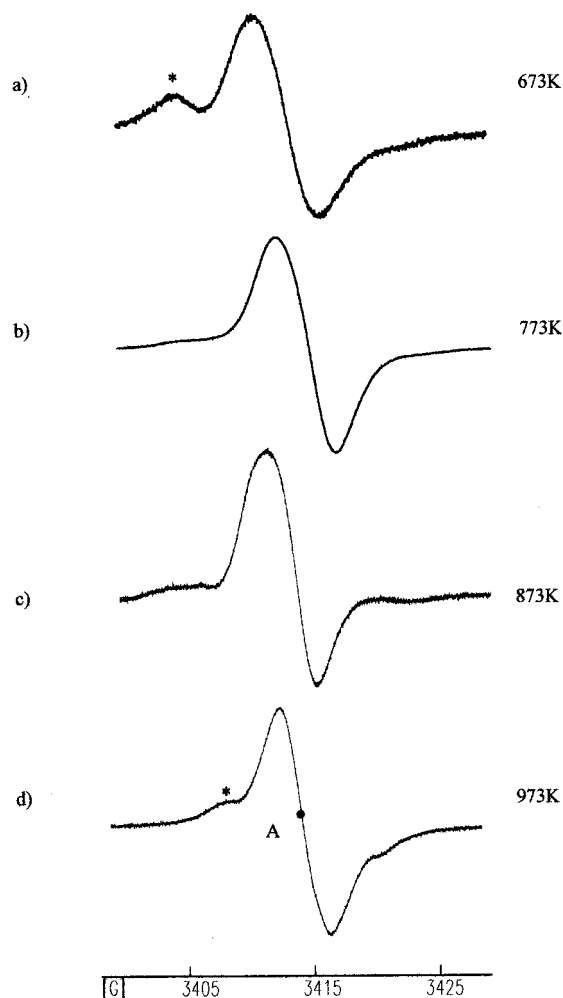


**Figure 5.** EPR spectra (100 K) of the color centers formed on MgO after UV irradiation under  $H_2$  on a sample dehydrated at (a) 673 K, (b) 773 K, (c) 873 K, and (d) 973 K.

$\Delta g$  shifts); (c) the immediate reactivity of the samples with molecular oxygen producing adsorbed superoxide radicals by electron transfer from the trapped electron center to dioxygen.

The line widths of the  $g \approx 2.000$  signal in Figure 5a–d are surprisingly large for surface  $F_S^+$  centers. This feature appears to be characteristic of the partially hydrated material, since the surface  $F_S^+(H)$  centers on the more thoroughly outgassed sample (Figure 1) have narrower line widths. After dehydration at 673–973 K, a significant abundance of residual surface OH groups is expected. Possible sources for the increased line width could therefore be due to a weak (unresolved) hyperfine interaction between the trapped electron of the color center and a neighboring OH group, or alternatively an inhomogeneously broadened line arising from an electron interaction with a number of surrounding OH groups. Neither possibility, however, appears to be the case based on the following observations.

The  $^1H$  ENDOR spectra of the partially dehydrated oxides are shown in Figure 6a–d. The spectra are dominated by the intense background  $^1H$  matrix signal which is now substantially broader compared to that obtained at higher activation temperatures (Figure 2). Although there are traces of a coupling in Figure 6d, one may conclude that there are no distinct and well resolved  $^1H$  couplings present, unlike the situation observed for the  $F_S^+(H)$  centers in Figure 2. In principle, a very weak coupling to a number of surrounding OH groups could occur so that the expected  $^1H$  coupling would be buried under the broad  $^1H$  matrix signal. This idea was tested by converting the

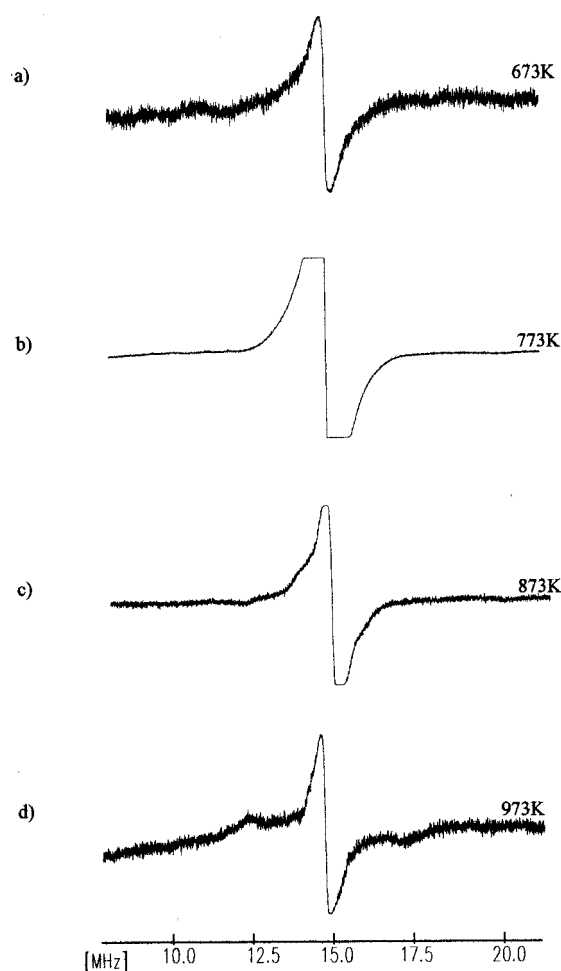


**Figure 6.** Corresponding  $^1H$  ENDOR spectra (100 K) of the surface color centers on MgO after dehydration at (a) 673 K, (b) 773 K, (c) 873 K, and (d) 973 K.

starting  $Mg(OH)_2$  powder to  $Mg(OD)_2$  using  $D_2O$ ; the sample was then activated at 873 K and UV irradiated (under  $D_2$ ) in the normal manner. As seen in Figure 7, the line shape and line width of the resulting EPR spectrum is similar in both cases, indicating that the broad line width does not originate from a hyperfine interaction with neighboring OH groups.

The most important information from the above results is as follows: (1) surface color centers are formed on partially hydrated MgO (673–973 K); (2) these color centers do not interact to any significant extent with the abundant surface OH groups; (3) the  $g$  values are slightly larger ( $g_{av} = 2.0008$ ) compared to those observed for the  $F_S^+(H)$  centers on the thoroughly dehydrated material (1023–1123 K; see Table 1).

**Superoxide ( $O_2^-$ ) Formation on MgO (673–1123 K).** Further information on the morphology of the defective MgO surface can be obtained by analysis of the EPR spectra of a suitable probe molecule, in this case the superoxide anion. Dioxygen is easily reduced to the corresponding anion  $O_2^-$  by reaction with the surface trapped electrons ( $F_S^+(H) + O_2 \rightarrow F_S^{2+}(H) + O_2^-$ ) producing a characteristic orthorhombic EPR spectrum with  $g_{xx} \neq g_{yy} \neq g_{zz}$ .<sup>34</sup> The magnitude of the  $g_{zz}$  component reflects the strength of the local crystal field, allowing the distinction among cations not only with the same nominal charge but also with different coordinative environments.<sup>34–36</sup> The resulting  $O_2^-$  spectra obtained after  $O_2$  adsorption on the F-center-containing samples (673–1123 K) are shown in Figure 8. The most important differences in this series of spectra are in the  $g_{zz}$  region. For MgO activated at 673 K (Figure 8a), a

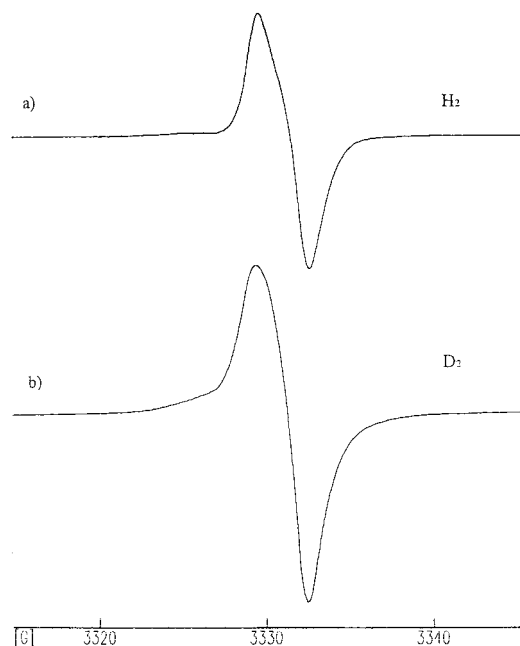


**Figure 7.** EPR spectra (100 K) of the surface color centers formed on (a) dehydration of  $\text{Mg}(\text{OH})_2$  at 873 K and subsequent UV irradiation under  $\text{H}_2$  and (b) dehydration of  $\text{Mg}(\text{OD})_2$  at 873 K and subsequent UV irradiation under  $\text{D}_2$ .

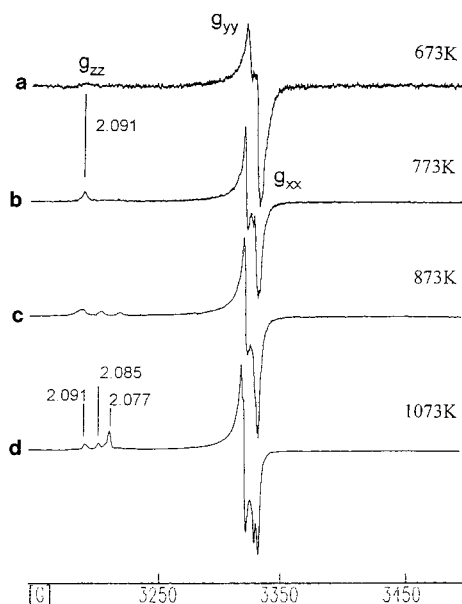


**Figure 8.** EPR spectra (100 K) of the superoxide radical ( $\text{O}_2^-$ ) on MgO containing surface color centers formed on the oxide dehydrated at various temperatures: (a) 673 K; (b) 773 K; (c) 873 K; (d) 1073 K.

high  $g_{zz}$  value of 2.091 dominates, while lower  $g_{zz}$  values (2.077 and 2.064) are observed on the samples activated at higher temperatures (873 and 1123 K; Figure 8, parts c and d).

Previous work on the EPR characterization of  $\text{O}_2^-$  adsorbed on fully dehydrated MgO assigned particular  $g_{zz}$  values to the  $\text{O}_2^-$  anion adsorbed at specific surface sites.<sup>34–36</sup> The highest  $g_{zz}$  component (2.091) was assigned to  $\text{O}_2^-$  adsorbed on a five-coordinated (hereafter indicated as 5C)  $\text{Mg}^{2+}$  cation on the planar (100) face of MgO, the 2.077 component to 4C  $\text{Mg}^{2+}$  cation at an edge site, and the remaining lower components to the anion adsorbed at lower coordinated sites which create stronger electrostatic potentials.<sup>34–36</sup> The results from Figure 8 indicate that on the partially hydrated sample (673 K) the  $\text{O}_2^-$  anions are stabilized almost exclusively on the planar (100)

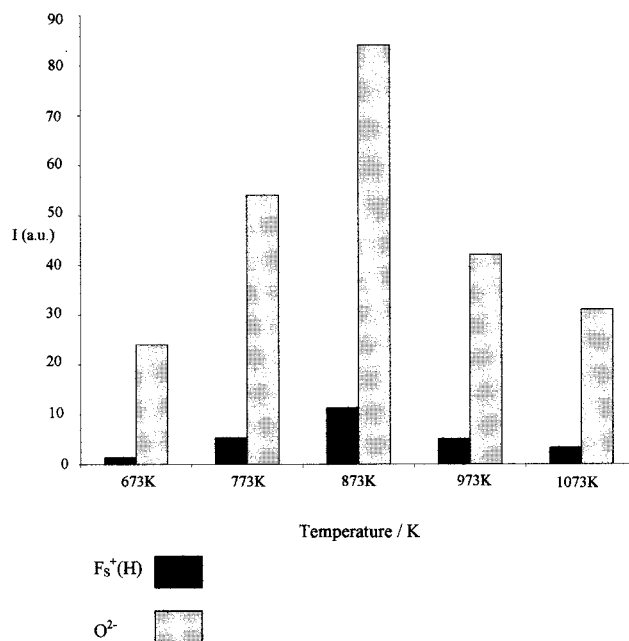


**Figure 9.** Relative integrated intensities of the paramagnetic surface color centers on MgO dehydrated at various temperatures and the corresponding superoxide ( $\text{O}_2^-$ ) intensities.

faces; the low coordinated sites which have a higher attractive potential for the anion are not available at this temperature. However, as the activation temperature is increased, progressive dehydroxylation occurs with resulting elimination of the bound OH groups from the low coordinated (4C and 3C) surface sites; these LC sites are now available for adsorption of the anion. Furthermore, the distribution of the  $g_{zz}$  components on the fully dehydrated sample (1123 K) indicates that low coordinated surface sites are clearly formed at these high temperatures.

The important conclusions from the superoxide spectra are (1)  $\text{O}_2^-$  anions are stabilized at the 5C  $\text{Mg}^{2+}$  cations on the (100) face of the partially dehydrated magnesia surface and, (2) on thoroughly dehydrated MgO, a variety of LC surface sites are present which stabilize the anion preferentially to the cations on the (100) face.

**Quantitative Aspects of Surface Defects.** The adsorbed  $\text{O}_2^-$  anion can provide not only qualitative information on the surface morphology (as discussed above) but also quantitative information on the number of trapped electrons available at the surface. Since the surface color centers will easily reduce most molecules to the corresponding radical anion,<sup>37–39</sup> dioxygen is easily converted to the superoxide anion ( $\text{O}_2^-$ ).<sup>34</sup> However, as one  $\text{O}_2^-$  anion is formed for every trapped electron present,<sup>34–37</sup> the *total* concentration of surface trapped electrons (both paramagnetic and diamagnetic) can be determined by double integration of the EPR spectra.

Diamagnetic surface color centers ( $\text{F}_s$  or  $\text{F}_s(\text{H})$  with two trapped electrons) are also formed by UV irradiation under  $\text{H}_2$  but are EPR silent; only the one-electron paramagnetic centers ( $\text{F}_s^+$  or  $\text{F}_s^+(\text{H})$ ) are visible. The relative integrated intensities for the paramagnetic  $\text{F}_s^+(\text{H})$  centers are presented in Figure 9. The lowest concentration of paramagnetic surface color centers is found on MgO dehydrated at 673 K. The concentration of these one electron trapped centers increases at higher temperatures, passing through a maximum at 873 K before decreasing again at the higher activation temperatures (1073 K).

The intensities of the corresponding superoxide spectra (Figure 8) are shown in Figure 9. One can clearly see that most of the color centers on the MgO surface exist in the diamagnetic

states. Nevertheless, the general trends in overall concentration remain the same, peaking at 873 K and decreasing again at higher temperatures. It is well-known that the surface area of the MgO changes as a function of the dehydration temperature, i.e., approximately  $280 \text{ m}^2 \text{ g}^{-1}$  (673 K),  $320 \text{ m}^2 \text{ g}^{-1}$  (773 K),  $300 \text{ m}^2 \text{ g}^{-1}$  (873 K),  $270 \text{ m}^2 \text{ g}^{-1}$  (973 K), and  $200 \text{ m}^2 \text{ g}^{-1}$  (1073 K).<sup>18</sup> The maximum surface area is therefore found after evacuation at 773 K. So the trends observed in Figure 9 are not entirely due to a surface area effect; they represent intrinsic changes to the defectivity of the surface.

To summarize the important points from the quantitative study, we may state that (1) high concentrations of surface color centers (anion vacancies) are formed on the partially hydrated MgO powders ( $T_{\text{dehy}} = 773$  and 873 K samples) and (2) the abundance of surface  $\text{F}_\text{S}^+(\text{H})$  ( $T_{\text{dehy}} = 1073$  K) centers is far less than the corresponding color centers on partially dehydrated MgO.

## Discussion

A thermally equilibrated crystal will possess a certain amount of disorder in the form of Schottky defects which consist of anion and cation vacancies in the bulk and surface phases of the crystal. While the total number of anion and cation vacancies in the crystal must be equal, it does not preclude defect concentration gradients between bulk and surface regions.<sup>17</sup> In the case of MgO,  $\text{O}^{2-}$  anion vacancies are the most common surface defects and they can be created in different ways. Vacuum annealing of MgO at very high temperatures (1473 K) results in surface oxygen removal,<sup>40</sup> while dehydration of the oxide at much lower temperatures (typically 873–1123 K,<sup>24,41</sup> but even as low as 773 K<sup>42</sup>) can also produce anion vacancies.

As mentioned in the Introduction, anion vacancies are intrinsically diamagnetic. However, if they trap a single electron, they become paramagnetic and can be conveniently studied by electron magnetic resonance techniques,<sup>18,25–33,43,44</sup> such as EPR and ENDOR. Since the order of stability of the defects is  $\text{F}_\text{S}^+ > \text{F}_\text{S}^{2+}$ , there is a strong attractive potential of the anion vacancies to trap an electron.<sup>11</sup> The presence of surface color centers on MgO (demonstrated by the above EPR spectra) signifies the presence of surface anion vacancies; these vacancies therefore undoubtedly exist on the oxide degassed in the temperature range 673–1123 K. However, the spectroscopic features of the color centers are quite different depending on the dehydration temperature, and this in turn indicates that the type or environment of the excess electron traps that are created varies as a function of the outgassing temperature. The following discussion will therefore examine the nature of the different color centers created at 1123, 1023–1073, and 673–973 K.

**The  $\text{F}_\text{S}^+(\text{H})$  I Center on MgO ( $T_{\text{dehy}} = 1123$  K).** At the highest dehydration temperature examined in this study (1123 K), one dominant surface color center exists. It is called the  $\text{F}_\text{S}^+(\text{H})$  center (labeled  $\text{F}_\text{S}^+(\text{H})$  I in Table 1). A detailed experimental and theoretical description of this defect was recently reported.<sup>25,26,28</sup> The most important points from these recent studies (with implications on the ensuing discussion below) may be summarized as follows.

(1) The electron trap responsible for the  $\text{F}_\text{S}^+(\text{H})$  center is regarded as an array of three equivalent  $\text{Mg}^{2+}$  ions formed by removal of a three-coordinated  $\text{O}^{2-}$  ion from the vertex of a cubic microcrystal, rather than the old model<sup>29–31</sup> which treated the vacancy as localized on the (100) face with resulting  $C_{4v}$  symmetry.

(2) The stabilization energy for the electron by the three cations at such a defect is surprisingly high and certainly larger than a hypothetical (100) vacancy trap.

(3) Rather than being an isolated point defect, the new vacancy may exist as part of an extended (111) polar face of the MgO crystal structure. Although electrically charged, stabilization of the electron may result in the favorable neutralization of the surface polarity.

The above assignment was based upon the combination of experimental<sup>28</sup> (EPR, FTIR, UV–vis spectroscopy) and theoretical data.<sup>11,28</sup> In particular, the well-known surface chemistry of chemisorbed  $\text{H}_2$  on the low coordinated surface anion–cation pairs of dehydroxylated MgO was instrumental in directing the assignment toward the low coordinated (3C) vacancy model. The anion vacancies formed at the latter stages of surface dehydroxylation are likely created at these corner positions in addition to the previously considered edge sites.<sup>24,26</sup> Three-coordinated MgO surfaces have been modeled in the past by a faceted (111) surface,<sup>12</sup> which was also observed experimentally,<sup>45,46</sup> indicating that hydroxylation occurs preferentially at these low coordination sites and even provides some stability for the crystal face.<sup>47,48</sup> Dehydroxylation and vacancy formation at these sites would then probably require the highest dehydration temperatures employed in this study, so it is reasonable to assume that these 3C vacancy traps (and  $\text{F}_\text{S}^+(\text{H})$  I centers) are almost exclusive to the thoroughly activated samples (1123 K). The low symmetry of this 3C color center, with a neighboring OH group, is also manifested in the symmetry of the EPR spectrum which is at least rhombic (as revealed by the ENDOR spectra where  $A_1 \neq A_2 \neq A_3$ ).

**Nature of the  $\text{F}_\text{S}^+(\text{H})$  II Centers on MgO ( $T_{\text{dehy}} = 1023$ –1073 K).** A second color center revealed by ENDOR and not previously reported was formed at the slightly lower dehydration temperatures of 1023–1073 K, labeled  $\text{F}_\text{S}^+(\text{H})$  II (Table 1). With the unmistakable proton coupling observed between the trapped electron and a neighboring OH group, this new defect can be formally classified as an  $\text{F}_\text{S}^+(\text{H})$  center, in analogy to the above  $\text{F}_\text{S}^+(\text{H})$  I species on MgO (1123 K).<sup>25,26,28</sup> However, there are some noted differences between this center (II) and the above-described  $\text{F}_\text{S}^+(\text{H})$  I center. In particular, (a) while  $\text{F}_\text{S}^+(\text{H})$  I dominates at high temperatures (1123 K),  $\text{F}_\text{S}^+(\text{H})$  II dominates at a slightly lower dehydration temperature (1023 K), as revealed by the trends in Figure 2; (b) the average  $g$  values are slightly larger compared to  $\text{F}_\text{S}^+(\text{H})$  I; (c) there is a noticeable smaller  $^1\text{H}$  coupling for species II. This previously unreported color center (II) can either be treated simply as a “modified”  $\text{F}_\text{S}^+(\text{H})$  I center on MgO  $T_{\text{dehy}} = 1123 \text{ K}$ <sup>25,26,28</sup> or it is an entirely new surface  $\text{F}_\text{S}^+(\text{H})$  species, containing an electron trapped in a different anion vacancy. It is not possible to make a definitive assignment at this stage as to the nature of this defect. However, on the basis of the above experimental data and knowledge about the surface dehydration process of MgO, some suggestions may be advanced.

The line width of the  $^1\text{H}$  ENDOR spectrum becomes noticeably broader at lower activation temperatures (see Figure 2). This could be explained as resulting from the increased heterogeneity associated with the surface morphology at lower temperature. In other words, as the surface defect sites become less well defined, the spectroscopic features could suffer as a broadening of the ENDOR lines. These arguments could be used to suggest that the second  $\text{F}_\text{S}^+(\text{H})$  II center is the very same  $\text{F}_\text{S}^+(\text{H})$  I center observed on MgO 1123 K, but now slightly “perturbed” by the increased heterogeneity of the surface or simply due to a slightly different position of the interacting OH group.

However, the above explanation does not account for all the facts, in particular the marked increased in concentration of



species II at lower temperatures (1023 K) and the smaller observed  $\Delta g$  shifts from  $g_e$  ( $g_{av} = 2.0004$  for center II compared to  $g_{av} = 1.9999$  for center I; Table 1). The  $g$  values of color centers depend on the spin-orbit coupling arising from an interaction with surrounding cations. As the interaction increases, the amount of  $p$  character admixed into the  $F_S^+$  wave function also increases, so negative  $\Delta g$  shifts occur ( $\Delta g = g - g_e$ ). Theoretical calculations clearly show a tendency for an increased interaction of the electron with surrounding surface cations on MgO (described by the magnitude of the  $^{25}\text{Mg}^{2+}$   $a_{iso}$  values) as the symmetry and coordination of the vacancy is reduced from  $C_{4v}$  (5C planar face) to  $C_{2v}$  (4C edge sites) and  $C_s$  (4C step sites); in other words, the unpaired spin is inhomogeneously distributed over the  $n$  cations around the vacancy due to the reduced empty space in the vacancy passing from 5C to 4C.<sup>26</sup> The  $g$  values of the center therefore depend primarily on the point symmetry and coordination of the vacancy itself and are less affected by the position of the interacting OH group. Since  $F_S^+(H)$  I has been assigned to a 3C corner vacancy and has large  $\Delta g$  shifts (1.9999), the  $F_S^+(H)$  II center with smaller  $\Delta g$  shifts (2.0004) could imply that the electron is trapped by a higher coordinated vacancy such as a 4C site. A variety of 4C-type anion vacancies can indeed exist on the dehydrated MgO surface, including edges and steps (monovacancy  $F_S^{2+}$  defects) or cation-anion vacancy pairs (divacancy  $P_S$  center), each of which can potentially trap and stabilize an electron.

The 4C monovacancies ( $F_S^{2+}$ ) should be very dominant on the dehydrated oxide surface. If we consider the process of vacancy formation by surface dehydration, Coluccia et al.<sup>22-24</sup> and Dunski et al.<sup>16</sup> have discussed in detail how low coordinated (4C) anion vacancies are created at the surface of polycrystalline MgO, involving the mobile surface proton and isolated OH groups located on edge sites, for example, as originally proposed by Peri<sup>49</sup> for alumina. These 4C edge vacancies are likely present on the MgO surface, in addition to the 3C corner vacancies responsible for the  $F_S^+(H)$  I site and can heterolytically chemisorb hydrogen as  $H^-$  and  $H^+$ . Upon UV irradiation, the adsorbed hydride releases an electron which will be subsequently stabilized in close proximity to the site of  $H^-$  adsorption<sup>28</sup> (i.e., at the low coordinated vacancy); it is less likely that the electron would migrate to a distant divacancy trap on the (100) face. Therefore, although the divacancies ( $P_S$  centers) may coexist with monovacancies on the fully dehydrated MgO surface and may even compete with  $F_S^{2+}$  centers as excess electron traps, the evidence points favorably toward the preferential trapping of the electron by low coordinated monovacancies present at edge, step, or corner sites (i.e., close to the  $H^-$  electron source). Indeed, the electron affinities for divacancies are generally much smaller compared to the isolated anion vacancies, and furthermore, while the first electron affinity is positive, the second is negative<sup>10</sup> (i.e.,  $F_S^{2+}$  acts as a better trap compared to  $P_S$ ). We suggest therefore that the second  $F_S^+(H)$  II center arises from an electron trapped in a 4C edge or step vacancy on MgO. If this is the case, the results indicate that the 4C vacancies are more abundant on the MgO surface dehydrated at 1023 K compared to MgO dehydrated at 1123 K where the  $F_S^+(H)$  I centers (3C vacancies) dominate. A schematic representation of the defects responsible for the  $F_S^+(H)$  centers I and II is shown in Figure 10.

**Nature of the Surface Defects on Partially Dehydrated MgO ( $T_{dehy} = 673-973$  K).** The EPR/ENDOR spectra of the partially hydrated samples do not display any visible  $^1H$  or  $^{25}\text{Mg}^{2+}$  hyperfine interactions. Without these "fingerprinting" characteristics, an accurate assignment of the paramagnetic

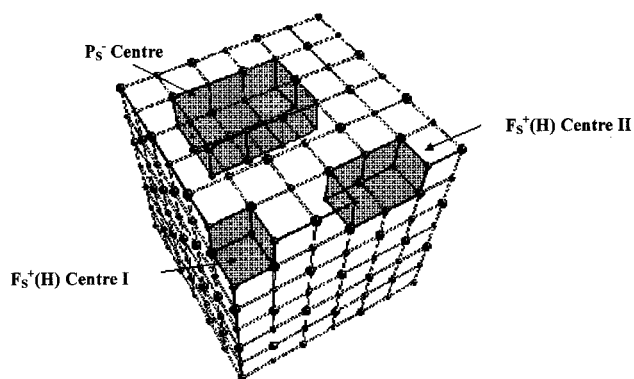


**Figure 10.** Schematic representation of the trapped electron centers on the surface of MgO. The different trapped electron centers predominate at different temperatures of activation; they are not all observed simultaneously:  $F_S^+(H)$  center I (dominant on MgO  $T_{dehy} = 1123$  K);  $F_S^+(H)$  center II (dominant on MgO  $T_{dehy} \approx 1048$  K); the suggested  $P_S^-$  divacancy (dominant on MgO  $T_{dehy} = 673-973$  K). The neighboring OH groups for centers I and II are not shown in the diagram.

defect based purely on the  $g$  values is more difficult. We shall therefore attempt to critically analyze the available data in conjunction with the existing knowledge about surface defects to propose some tentative assignments.

There is ample evidence in the literature to suggest that point defects are present on partially dehydrated MgO surfaces. Over pure MgO, activated at 773 K, intrinsic cation vacancies are formed which react with molecular oxygen to form  $O^-$  centers; the latter anions are responsible for H abstraction from methane to produce methyl radicals.<sup>50</sup> Furthermore, the electronic holes  $O^-$  are known to be easily stabilized by the presence of  $\text{Mg}^{2+}$  vacancies<sup>51,52</sup> and low coordinated surface sites.<sup>52</sup> TEM studies of HSA MgO prepared by decomposition of the hydroxide at low temperature (473 K) have also demonstrated that high index planes (like (111), (110), and (200)) prevail on such surfaces as compared to the stable (100) surface planes.<sup>54,55</sup> Thermal treatment above 673 K then initiates not only dehydroxylation but also irreversible structural rearrangements which transform the original unstable high index planes into the stable (100) planes.<sup>56</sup> It is also reported that the thermal decomposition of magnesium hydroxide involves a topotactic transformation in which some of the morphological features of the precursor crystals are retained.<sup>57,58</sup> The coordinative unsaturation of the  $\text{Mg}^{2+}$  cations will therefore be retained in the low (temperature) product oxide in addition to coordinatively unsaturated  $O^{2-}$  ions. This implies the presence of structural defects in the resulting MgO powder, after low-temperature decomposition of the hydroxide, which are intrinsic to the precursor hydroxide state.<sup>59</sup> Ito et al.<sup>41</sup> have also observed that preirradiation of MgO ( $T_{dehy} = 723$  K) with UV light produces surface  $O^-$  species which subsequently react with  $H_2$  to form surface  $F_S^+$  color centers. They suggested that the hydrogen molecule is homolytically dissociated on the surface  $O^-$  anions.<sup>40</sup> It was proposed that the irradiation-induced active sites on these samples were aggregations of four  $O_{4C}^{2-}$  (i.e., a surface cation vacancy) and of four  $\text{Mg}_{4C}^{2+}$  ions (i.e., a surface anion vacancy).<sup>41</sup> The picture emerging from these and similar studies is that the partially dehydrated MgO surface (600–1000 K) undergoes complex morphological transformations where monovacancies such as anion and cation defects, and possibly pairs of these defects (divacancies), certainly exist even at "relatively" low temperatures. In other words, one does not strictly require elevated dehydration temperatures to produce electron trapping sites at the magnesia surface.



Lunsford and Jayne<sup>18</sup> originally investigated the nature of the surface defects formed on partially and fully dehydrated polycrystalline magnesite. In confirmation with the above results, they observed similar EPR spectra over the same temperature range and ascribed them to surface color centers. Color centers labeled "S<sub>2</sub> centers" were formed on samples degassed at 873 K, and color centers labeled "S' centers" were formed on the 1073 K dehydrated surfaces. The S<sub>2</sub> center on partially dehydrated MgO was assigned to an electron trapped in a monovacancy ( $F_s^{2+} + e^- \rightarrow F_s^+$ ), while the S' center formed on the fully dehydrated material was assigned to an electron trapped by a cation-anion vacancy pair. Ojamäe and Pisani<sup>10</sup> have recently performed theoretical calculations on such a divacancy model as a potential electron trapping site on the (100) surface of MgO. They suggest that the divacancy is a common defect, if not the most common, at the highly dehydrated MgO surface, since the formation energy of the divacancy from two charged isolated vacancies is very high (300 kcal/mol).<sup>10</sup> Furthermore, the electron trapped in a neutral divacancy with a neighboring proton is neutral and can be present in high concentrations without the need for compensating charges.<sup>10</sup>

On fully dehydrated MgO, the source of electrons for the  $F_s^+(H)$  color centers originates exclusively from adsorbed hydrides; so although divacancies may be present, most of the physicochemical transformations associated with color center formation occur at low coordinated surface sites. However, at low dehydration temperatures, these low coordinated surface sites which heterolytically adsorb dihydrogen are effectively "blocked" by OH groups and cannot partake in the interesting chemistry of H<sub>2</sub> chemisorption. In the absence of low coordinated 4C and 3C monovacancies, which are heavily hydroxylated and therefore almost "inert" to H<sub>2</sub> chemisorption, the divacancies would represent the next most likely electron traps. At these low dehydration temperatures, the OH groups from the (100) face of the oxide have already been eliminated,<sup>16,22-24</sup> so in principle the hypothetical divacancy on the (100) face, suggested by Lunsford and Jayne<sup>18</sup> and Ojamäe and Pisani,<sup>10</sup> may be free of surrounding OH groups. This would explain the absence of any observable <sup>1</sup>H coupling in the ENDOR spectrum of the color centers on the partially dehydrated surfaces (Figure 6). These color centers would easily reduce oxygen to the superoxide radical, which would subsequently be stabilized at the closest available Mg<sup>2+</sup> cation, in this case the surrounding 5C Mg<sup>2+</sup> cations on the (100) face. The superoxide spectra therefore provide additional evidence for the location of the vacancies on the planar (100) face of the oxide.

Experimental evidence in the literature indicates that cation-anion vacancies are formed on the partially dehydrated MgO surface; to the best of our knowledge, there is no direct experimental evidence to suggest that they are present on completely dehydrated surfaces. In conjunction with the above discussions, we therefore suggest that the color centers formed on the partially dehydrated surface may be assigned to divacancy  $P_s^-$  centers. A schematic illustration of the divacancy is shown in Figure 10.

Two final points on the discussion of the proposed  $P_s^-$  centers concern their mechanism of formation and their apparent absence at higher activation temperatures. The source of electrons for formation of these paramagnetic centers remains uncertain. Ito et al.<sup>41</sup> suggested that over UV-irradiated MgO ( $T_{\text{dehy}} = 723$  K) the low coordinated surface  $O^{2-}$  anions are ionized ( $O^{2-} + h\nu \rightarrow O^- + e^-$ ) and the released electrons become subsequently trapped at a surface anion vacancies ( $e^- + F_s^{2+} \rightarrow F_s^+$ ). In other words, H<sub>2</sub> is not necessary as a source

of electrons. Subsequent adsorption of H<sub>2</sub> however will produce additional trapped electrons as the molecule is homolytically split over the surface O<sup>-</sup> anions ( $O^- + H_2 + O^{2-} \rightarrow 2OH^- + e^-$ ), and as before, the released electrons are stabilized by the anion vacancies ( $e^- + F_s^{2+} \rightarrow F_s^+$ ). If this mechanism is correct, then only a fraction of the color centers formed on the partially hydrated samples (673–973 K) would be expected to have an observable superhyperfine interaction with a neighboring OH group, explaining the absence of the <sup>1</sup>H coupling by ENDOR. Further work is required by other techniques to clarify the mechanism of color center formation over the partially hydrated materials. The apparent absence of these color centers at higher dehydration temperatures may be explained by considering a dynamic view of the MgO surface in which the morphology changes with temperature, as discussed below.

**"Dynamic" Aspects of MgO Morphology.** One outstanding point from the above work concerns the relative distributions of type I (3C) and type II (4C)  $F_s^{2+}$  vacancies on MgO at different temperatures. As seen in Figure 2, the  $F_s^+(H)$  centers are quite abundant on MgO 1048 K (Figure 2b) and still visible at 1073 K (Figure 2c). Nevertheless, under high activation conditions (1123 K), this defect is no longer visible. Indeed, the overall concentration of surface trapped electrons has diminished somewhat (Figure 9), and only the  $F_s^+(H)$  centers remain visible at 1123 K. Even though the relative stability of oxygen vacancies at low coordinated sites is theoretically greater compared to the high coordinated sites,<sup>11</sup> (i.e.,  $F_s^+(H)$  I should be slightly more stable than  $F_s^+(H)$  II) one would still expect to see traces of the second II species in the spectrum. This is not the case, suggesting that the 4C edge sites are no longer present on the surface at the highest activation temperature.

This fact could be accounted for by considering a dynamic view of the MgO morphology, which changes markedly as a function of temperature. Pacchioni and Pescarmona<sup>11</sup> have recently investigated oxygen migration for  $F_s^{2+}$  defects on MgO and demonstrated that migration can occur from low coordinated sites to high coordinated sites. If this occurs at elevated temperatures on the thoroughly dehydrated oxide, the observed low coordinated defects (I and II) may migrate from the chemically reactive edge and corner sites to the less reactive high coordinated sites. Notwithstanding the decrease in surface area, this would account for the overall decrease in type I and II centers at high temperatures. The hypothetical divacancies abundant at low temperatures, may also be destroyed at the higher activation temperatures when the surface area of the oxide is dramatically reduced, as the surface undergoes major reconstructions. This would account for the apparent absence of the signal due to the possible  $P_s^-$  centers on the thoroughly dehydrated samples (Figures 1 and 2).

The results show that there is not one simple and static view of the MgO surface. Instead, one must consider the dynamic changes which accompany the dehydration and activation of the oxide, from low temperatures (during which the hydroxide is converted to the oxide) to high temperatures (during which the fully formed oxide phase experiences changes in surface area and migration of surface point defects). Despite its simplicity, the surface of the oxide varies dramatically as a function of temperature so that it is not always a trivial task to reproduce and interpret theoretical and experimental data on MgO morphology.

## Conclusions

Dehydration of MgO over a range of temperatures (673–1123 K) results in the formation of surface point defects. These

defects can be subsequently populated with electrons by UV irradiation of the oxide under  $H_2$ . The distribution and type of vacancies formed and the likelihood that the vacancies trap an electron depends critically however on the dehydration temperature.

On partially dehydrated MgO (673–973 K), paramagnetic divacancy color centers ( $P_S^-$ ) most probably dominate. At these low temperatures, the low coordinated edge, step, and corner cation–anion pairs are effectively “blocked” by surface hydroxyls and cannot participate in the heterolytic chemisorption of hydrogen, a prerequisite for the formation of the monovacancy  $F_S^+(H)$  type color centers. In the absence of these low coordinated sites, the chemistry of color center formation occurs around the surface divacancies on the (100) face. The mechanism of color center formation is not completely understood in this case but is likely different from the heterolytic adsorption processes which occur on fully dehydrated MgO. Due to the ease of removal of surface OH groups from the (100) face, there is no observable  $^1H$  coupling associated with the divacancy  $P_S^-$  center due to the absence of surrounding OH groups.

On thoroughly dehydrated MgO, a variety of potential excess electron-trapping sites likely exist. However, not all are equally populated with electrons. The low coordinated cation–anion pairs are completely dehydroxylated and can reversibly and irreversibly coordinate  $H^-$  species, which upon UV irradiation produce surface  $F_S^+(H)$ -type centers. Two types of surface  $F_S^+(H)$  centers have been observed by ENDOR spectroscopy and have been assigned to an electron trapped in a 3C corner and 4C edge (or step) monovacancy defect.

Whatever the precise description on the nature of the point defects formed on MgO, it is clear from the above work that the morphology and heterogeneity of even the simplest of binary oxides remains poorly understood, particularly for the partially dehydrated surface. Although the reactivity of simple probe molecules with thoroughly dehydroxylated MgO has received significant attention experimentally and theoretically, the chemistry occurring on the partially hydroxylated material may be significantly different. Considering most practical applications of magnesia utilize the material under hydrated/partially hydrated conditions, more research is needed before a comprehensive description of the polycrystalline oxide surface is available.

**Acknowledgment.** Financial support for the National ENDOR Centre at Cardiff University from the EPSRC is gratefully acknowledged. D.M.M. thanks Dr. A. Ponti, Università di Milano, for helpful technical suggestions.

## References and Notes

- Heinrich, V. E.; Cox, P. A. *The Surface Science of Metal Oxides*; Cambridge University Press: Cambridge, 1994.
- Colburn, E. A. *Surf. Sci.* **1992**, *15*, 281.
- Shluger, A. L.; Gale, J. D.; Catlow, C. R. A. *J. Phys. Chem.* **1992**, *96*, 10389.
- Wu, M. C.; Truong, C. M.; Coulter, K.; Goodman, D. W. *J. Am. Chem. Soc.* **1992**, *114*, 7565.
- Gibson, A.; Haydock, R.; LaFemina, J. P. *Phys. Rev. B* **1994**, *50*, 2582.
- Ferrari, A. M.; Pacchioni, G. *J. Phys. Chem.* **1995**, *99*, 17010.
- Kantorovich, L. N.; Holender, J. M.; Gillan, M. J. *Surf. Sci.* **1995**, *343*, 221.
- Ferrari, A. M.; Pacchioni, G. *J. Phys. Chem.* **1996**, *100*, 9032.
- Scorza, E.; Birkenheuer, U.; Pisani, C. *J. Chem. Phys.* **1997**, *107*, 9645.
- Ojamae, L.; Pisani, C. *J. Chem. Phys.*, in press.
- Pacchioni, G.; Pescarmona, P. P. *Surf. Sci.*, in press.
- de Leeuw, N. H.; Watson, G. W.; Parker, S. C. *J. Chem. Soc., Faraday Trans.* **1996**, *92*, 2081.
- Parker, S. C.; Oliver, P. M.; De Leeuw, N. H.; Titiloye, J. O.; Watson, G. W. *Phase Transitions* **1997**, *61*, 83.
- Picaud, S.; Hoang, P. N. M.; Girardet, C. *Surf. Sci.* **1992**, *278*, 339.
- Goniakowski, J.; Noguera, C. *Surf. Sci.* **1995**, *330*, 337.
- Dunski, H.; Jozwaik, W. K.; Sugier, H. *J. Catal.* **1994**, *146*, 166.
- Harkins, C. G.; Shang, W. W.; Leland, T. W. *J. Phys. Chem.* **1969**, *73*, 130.
- Lunsford, J. H.; Jayne, J. P. *J. Phys. Chem.* **1966**, *70*, 3464.
- Kawakami, H.; Yoshida, S. *J. Chem. Soc., Faraday Trans. 2* **1984**, *80*, 921.
- Jones, C. F.; Reeve, R. A.; Rigg, R.; Segal, R. L.; Smart, R. St. C.; Turner, P. S. *J. Chem. Soc., Faraday Trans. 1* **1984**, *80*, 2609.
- Duley, W. J. *J. Chem. Soc., Faraday Trans. 1* **1984**, *80*, 1173.
- Coluccia, S.; Boccuzzi, F.; Ghiotti, G.; Morterra, C. *J. Chem. Soc., Faraday Trans. 1* **1982**, *78*, 2111.
- Coluccia, S.; Marchese, L.; Lavagnino, S.; Anpo, M. *Spectrochim. Acta* **1987**, *43A*, 1573.
- Coluccia, S.; Lavagnino, S.; Marchese, L. *Mater. Chem. Phys.* **1988**, *18*, 445.
- Giamello, E.; Murphy, D. M.; Ravera, L.; Coluccia, S.; Zecchina, A. *J. Chem. Soc., Faraday Trans.* **1994**, *90*, 3167.
- Giamello, E.; Paganini, M. C.; Murphy, D. M.; Ferrari, A. M.; Pacchioni, G. *J. Phys. Chem.* **1997**, *101*, 971.
- Chiesa, M.; Paganini, M. C.; Giamello, E.; Murphy, D. M. *Langmuir* **1997**, *13*, 5306.
- Paganini, M. C.; Chiesa, M.; Giamello, E.; Martra, G.; Coluccia, S.; Murphy, D. M.; Pacchioni, G. *Surf. Sci.*, in press.
- Tench, A. J.; Nelson, R. L. *J. Colloid Interface Sci.* **1968**, *26*, 364.
- Nelson, R. L.; Tench, A. J.; Harmsworth, B. J. *Trans. Faraday Soc.* **1967**, *63*, 1427.
- Tench, A. J.; Nelson, R. L. *Trans. Faraday Soc.* **1967**, *63*, 2254.
- Spaeth, J. M.; Niklas, J. R.; Bartram, R. H. *Structural Analysis of Point Defects in Solids: Introduction to Multiple Magnetic Resonance Spectroscopy*; Springer: Heidelberg, 1992.
- Sothe, H.; Jordan, M.; Spaeth, J. M. *J. Phys.: Condens. Mater.* **1993**, *5*, 1957.
- Giamello, E.; Murphy, D. M.; Garrone, E.; Zecchina, A. *Spectrochim. Acta* **1993**, *49A*, 1323.
- Giamello, E.; Garrone, E.; Ugliengo, P. *J. Chem. Soc., Faraday Trans. 1* **1989**, *85*, 1373.
- Giamello, E.; Garrone, E.; Ugliengo, P.; Che, M.; Tench, A. J. *J. Chem. Soc., Faraday Trans. 1* **1989**, *85*, 3987.
- Giamello, E.; Murphy, D. M.; Marchese, L.; Martra, G.; Zecchina, A. *J. Chem. Soc., Faraday Trans.* **1993**, *89*, 3715.
- Giamello, E.; Murphy, D. M. In *Radicals on Surfaces*; Lund, A., Rhodes, C., Eds.; Topics in molecular Organisation and Engineering 13; Kluwer Academic Publications: Norwell, 1995; p 147.
- Giamello, E.; Paganini, M. C.; Murphy, D. M. *Colloids Surf.* **1996**, *115*, 157.
- Wertz, J. E.; Orton, J. W.; Auzins, P. *J. Appl. Phys.* **1962**, *33*, 322.
- Ito, T.; Kawanami, A.; Toi, K.; Shirakawa, T.; Tokuda, T. *J. Phys. Chem.* **1988**, *92*, 3910.
- Winter, E. R. S. *Adv. Catal.* **1958**, *10*, 196.
- Weber, H. Z. *Phys.* **1951**, *130*, 392.
- Wertz, J. E.; Auzins, P.; Weeks, R. A.; Silsbee, R. H. *Phys. Rev.* **1957**, *107*, 1535.
- Henrich, V. E. *Surf. Sci.* **1976**, *57*, 385.
- Onishi, H.; Egawa, C.; Aruga, T.; Iwasawa, Y. *Surf. Sci.* **1987**, *191*, 479.
- Rohr, F.; Wirth, K.; Libuda, J.; Cappus, D.; Bamer, M.; Freund, H. *Surf. Sci.* **1994**, *977*, 315.
- Pojani, A.; Finocchi, F.; Goniakowski, J.; Noguera, C. *Surf. Sci.* **1997**, *387*, 354.
- Peri, J. B. *J. Phys. Chem.* **1965**, *69*, 220.
- Driscoll, D. J.; Martir, W.; Wang, J. X.; Lunsford, J. H. *J. Am. Chem. Soc.* **1985**, *107*, 58.
- Pope, S. A.; Guest, M. F.; Hillier, I. H.; Colburn, E. A.; Mackrodt, W. C.; Kendrick, J. K. *Phys. Rev. B* **1983**, *28*, 2191.
- Johnson, M. A.; Stefanovich, E. V.; Truong, T. N.; *J. Phys. Chem. B* **1997**, *101*, 3196.
- Kobayashi, H.; Salahub, D. R.; Ito, T. *J. Phys. Chem.* **1994**, *98*, 5487.
- Moodie, A. F.; Warble, C. E. *J. Cryst. Growth* **1971**, *10*, 26.
- Coluccia, S.; Tench, A. J.; Segall, R. J. *J. Chem. Soc., Faraday Trans. 1* **1979**, *75*, 1769.
- Knozinger, E.; Jacob, K.-H.; Singh, S.; Hofmann, P. *Surf. Sci.* **1993**, *290*, 388.
- Moodie, A. F.; Warble, C. E. *J. Cryst. Growth* **1986**, *74*, 89.
- Ribeiro Carrot, M. M. L.; Carrott, P. J. M.; Brotas de Carvalho, M. M.; Sing, K. S. W. *J. Chem. Soc., Faraday Trans. 1* **1991**, *87*, 185.
- Ribeiro Carrott, M.; Carrott, P.; Brotas de Carvalho, M.; Sing, K. S. W. *J. Chem. Soc., Faraday Trans. 1* **1993**, *89*, 579.